Therapeutic effects of KCC2 chloride transporter activation on detrusor overactivity in mice with spinal cord injury

1 **Therapeutic effects of KCC2 chloride transporter activation on detrusor**

2 **overactivity in mice with spinal cord injury**

3

4 Kyohei Watanabe[1)2)], Masaru Ishibashi[1)], Takahisa Suzuki[3)4)], Atsushi Otsuka[2)],

5 Naoki Yoshimura[5)], Hideaki Miyake[2)], and Atsuo Fukuda[1)]

6

7 1 Department of Neurophysiology, Hamamatsu University School of Medicine,

8 Hamamatsu, Japan

9 2 Department of Urology, Hamamatsu University School of Medicine,

10 Hamamatsu, Japan

11 3 Department of Urology, Kanagawa Rehabilitation Hospital, Atsugi, Japan

12 4 Department of Urology, Yokohama City University, Yokohama, Japan

13 5 Department of Urology, University of Pittsburgh School of Medicine, Pittsburgh,

14 PA, USA

15

16

17 Correspondence: Atsuo Fukuda, M.D., Ph.D.

18 Department of Neurophysiology, Hamamatsu University School of Medicine,

19 Hamamatsu, Japan

20 1-20-1 Handayama, Higashi-Ku, Hamamatsu, Japan 431-3192

21 Tel.: +81-53-435-2246, Fax: +81-53-435-2245

22 E-mail: axfukuda@hama-med.ac.jp

23

24

25

1

26 **Running Title**

28

29

30 **ABSTRACT**

31 This study aimed to clarify whether the down regulation of K+-Cl−co-transporter
32 2 (KCC2) in the sacral parasympathetic nucleus (SPN) of the lumbosacral spinal
33 cord, from which the efferent pathway innervating the bladder originates, causes
34 cellular hyperexcitability and triggers detrusor overactivity (DO) in spinal cord
35 injury (SCI). SCI was produced by the Th8-9 spinal cord transection in female
36 C57BL/6 mice. At 4 weeks after SCI, CLP290, a KCC2 activator, was
37 administered, and cystometry was performed. Thereafter, neuronal activity with
38 c-fos staining and KCC2 expression in the cholinergic preganglionic
39 parasympathetic neurons in the SPN were examined using
40 immunohistochemistry. Firing properties of neurons in the SPN region were
41 evaluated by extracellular recordings in spinal cord slice preparations. DO
42 evident as non-voiding contractions (NVC) was significantly reduced by CLP290
43 treatment in SCI mice. The number of c-fos-positive cells and co-expression of
44 c-fos in choline acetyltransferase (ChAT)-positive cells were decreased in the
45 SPN region of SCI-CLP290 group vs. SCI-vehicle group. KCC2
46 immunoreactivity was present on the cell membrane of SPN neurons, and the
47 normalized fluorescence intensity of KCC2 in ChAT-positive SPN neurons was
48 decreased in SCI-vehicle group, vs. SI-vehicle group, but recovered in
49 SCI-CLP290 group. Extracellular recordings showed that CLP290 suppressed
50 the high frequency firing activity of SPN neurons in SCI mice. These results
51 indicated that SCI-induced DO is associated with downregulation of KCC2 in
52 preganglionic parasympathetic neurons, and that activation of KCC2
53 transporters can reduce DO, increase KCC2 expression in preganglionic
54 parasympathetic neurons and decrease neuronal firing of SPN neurons in SCI
55 mice.

56

57

58 NEW & NOTEWORTHY

59 This study is the first report to suggest that activation of KCC2 chloride ion

60   transporter may be a therapeutic modality for the treatment of SCI-induced DO

61   by targeting bladder efferent pathways.

62

63   Key words: KCC2, detrusor overactivity, efferent nerve, sacral parasympathetic

64   nucleus, spinal cord injury

65

66   Abbreviations:

67   BDNF: brain-derived neurotropic factor

68   ChAT: choline acetyltransferase

69   DO: detrusor overactivity

70   DCM: dorsal commissure

71   GABA: gamma-aminobutyric acid

72   ICI: intercontraction interval

73   IHC: immunohistochemistry

74   IVBP: intravesical baseline pressure

75   KCC2: K^+-Cl^- co-transporter2

76   LDH: lateral dorsal horn

77   LUTD: lower urinary tract dysfunction

78   MCP: maximum voiding bladder contraction pressure

79   MDH: medial dorsal horn

80   NVCs: Non-voiding contractions

81   OAB: overactive bladder

82   PVR: post-void residual urine volume

83   QOL: quality of life

84   SCI: spinal cord injury

3

85   SI: spinal intact

86   SPN: sacral parasympathetic nucleus

87

88

INTRODUCTION

Overactive bladder (OAB) is generally characterized by frequent urination, urgency, and urge urinary incontinence, that impairs quality of life [1]. The main mechanism underlying the pathophysiology of OAB is detrusor overactivity (DO), which produces involuntary contractions of the detrusor muscles during the urine storage phase [2].

The functions of the lower urinary tract depend on the coordination of neural circuits in the brain, spinal cord, and peripheral nervous system, and several neurotransmitters play important roles in the control of these functions [3]. Spinal cord injury (SCI) above the sacral level has been identified as one of the major disorders inducing lower urinary tract dysfunction (LUTD), including DO [4]. Although various mechanisms have been reported for SCI-induced DO, previous studies showed that gamma-aminobutyric acid (GABA) and glycine, two major inhibitory neurotransmitters in the central nervous system (CNS), were down-regulated in the lumbosacral spinal cord after SCI, as evidenced by the reduced expressions of the GABA-synthesizing enzyme, glutamic acid decarboxylase (GAD) [5] and glycine [6], respectively.

Furthermore, GABA generally exerts inhibitory effects in the CNS, including the spinal cord; however, it may also act as an excitatory transmitter in immature cells or under pathological conditions, such as injury [7][8][9]. This paradoxical signaling of GABA is dependent on the intracellular Cl^- concentration in neurons. K^+-Cl^- co-transporter 2 (KCC2) is specifically expressed in nerve cells, and maintains a low intracellular Cl^- concentration by pumping K^+ and Cl^- ions out of the cell [10]. Therefore, when KCC2 levels are low, for example, during the developmental phase, intracellular Cl^- concentrations are high. As a consequence, the activation of $GABA_A$ or glycine receptors at inhibitory

5

116 synapses causes Cl$^-$ ions to flow out of cells, thereby inducing the membrane

117 depolarization of postsynaptic neurons to exert excitatory effects rather than

118 inhibitory effects [8]. In the post-developmental state, KCC2 levels are highly

119 up-regulated to maintain a low intracellular Cl$^-$ concentration; therefore, the

120 activation of GABA$_A$ or glycine receptors causes Cl$^-$ ions to flow into cells and

121 exert inhibitory effects on postsynaptic neurons [8][9][10]. However, under

122 pathological conditions, such as neuropathic pain and epilepsy, the

123 hyperexcitatory response during GABA$_A$/glycine receptor activation reportedly

124 re-emerges due to the down-regulation of KCC2 [11][12][13]. Based on these

125 findings, the down-regulation of KCC2 appears to cause functional abnormalities

126 in the micturition pathway. SCI has been shown to reduce the expression of

127 KCC2 in the rat lumbar spinal cord and cause disinhibition, resulting in spasticity

128 [14]. However, the role of KCC2 in SCI-induced DO is still unknown. Therefore,

129 the present study investigated whether the disruption of intracellular Cl$^-$

130 homeostasis associated with changes in KCC2 expression contributes to the

131 formation of hyper-excitatory responses, such as DO, in the spinal micturition

132 neural circuitry after SCI. We focused on SCI-induced changes in spinal

133 autonomic preganglionic neurons that control bladder function through

134 parasympathetic efferent pathways because these neurons reportedly receive

135 direct inhibitory inputs from GABAergic interneurons in the lumbosacral spinal

136 cord [15][16].

137

138 **Materials and Methods**

139 Animals

140 We used female C57BL/6 mice (8-9 weeks old; body weight of approximately

141 17-20 g, and 3-4 weeks old; body weight of 9-15 g) purchased from SLC

142 (Shizuoka, Japan). After 4 weeks, the former group of mice were used for

6

143   cystometry (n=40 total; n=10 per group) and immunohistochemistry at 12-13

144   weeks old (n=15 total; n=5 per group), while the latter was used for

145   electrophysiological experiments (n=22 total; SI mice: n=5, SCI mice: n=7, SCI

146   control: n=5 and SCI CLP290: n=5) at 7-8 weeks old. Mice were housed in

147   cages under a 12-hour light-dark cycle (lights off from 1900 to 0700) and were

148   allowed free access to drinking water and food pellets. All experiments were

149   performed in accordance with the guidelines issued by the Hamamatsu

150   University School of Medicine for the ethical use of animals for experimentation,

151   and all efforts were made to minimize the number of animals used and their

152   suffering.

153

154   Spinal cord surgery

155   Animals were randomly divided into SI and SCI subgroups. SCI mice were

156   created by complete transection of the Th8-9 spinal cord under 2% isoflurane

157   anesthesia. In the control group of spinal cord intact (SI) mice, the back muscle

158   incision was similarly made and sutured as sham surgery without any further

159   procedure. Antibiotics (150 mg/kg ampicillin) were administered 1 hour after

160   surgery and the day after surgery. Since the SCI group had postoperative urinary

161   retention, the bladder was emptied by manually compressing the abdominal wall

162   once daily for 4 weeks postoperatively until the final experiment. In the four

163   weeks after surgery, SCI mice developed a spinally-mediated new voiding reflex

164   with involuntary contractions of the bladder [3]. We randomly divided mice into

165   four different groups: sham surgery with vehicle administration (SI-vehicle),

166   sham surgery with CLP290 administration (SI-CLP290), SCI with vehicle

7

167 administration (SCI-vehicle), and SCI with CLP290 administration

168 (SCI-CLP290).

169

170 Drugs

171 The dose and method of drug administration were selected according to a

172 previous study [17]. CLP290, which is a potent activator of KCC2, was dissolved

173 in 123.62 mM dimethyl sulfoxide (DMSO) and 20%

174 2-hydroxypropyl-β-cyclodextrin, and the final dose was set to 100 mg/kg for oral

175 administration. CLP290 was administered in a single dose during each

176 experiment and the vehicle was used for control conditions.

177

178 Cystometry

179 Using SI and 4-week SCI mice (8-9 weeks old before surgery), cytometry was

180 performed under awake conditions. After anesthesia with 2% isoflurane, a

181 midline incision in the lower abdomen exposed the bladder. An SP-45 tube

182 (Natsume Seisakusho), the end of which was flared with heat, was inserted

183 through a small incision in the bladder dome, secured to the bladder with a

184 drawstring suture, and the skin wound was then closed with sutures. Mice were

185 placed in Tube Rodent Holders (Kent Scientific Corporation), and the intravesical

186 catheter was connected to a pressure transducer and syringe pump connected

187 to the PowerLab system (AD Instruments). After recovery from anesthesia,

188 which was confirmed by avoidance behavior induced by forepaw pinches, saline

189 was continuously instilled into the bladder (0.01 ml/min). After the initiation of the

190 intravesical instillation and the achievement of a stable bladder pressure

8

191   waveform, vehicle or CLP290 was administered to SI and SCI mice. Cystometric

192   recordings were re-started from 1 hour after vehicle or drug administration, at

193   which time the highest blood concentration of CLP290 was reportedly achieved

194   [17]. We measured intercontraction intervals (ICI), maximum voiding bladder

195   contraction pressure (MCP), intravesical baseline pressure (IVBP), post-void

196   residual urine volume (PVR), and non-voiding contractions (NVCs) counted for 1

197   hour. As reported in previous studies, ICI is the average of intervals between two

198   consecutive peaks, and PVR was measured as the amount of urine collected

199   with micro-syringe aspiration after the last voiding contraction. NVCs were

200   defined as small-amplitude bladder contractions more than 6 cmH_2O above the

201   baseline without saline leakage during the storage phase [3]. Parameters of

202   cystometry were determined at average of wave in several times.

203

204   Immunohistochemistry

205   The immediate early gene, c-fos, one of transcription factors, was used as a

206   marker of neuronal activity indicating postsynaptic activation of

207   micturition-related spinal cord neurons under SCI conditions [18]. Previous

208   studies reported the maximal expression of c-fos in the spinal cord 2 hours after

209   the intravesical infusion of saline [19]; therefore, tissues were harvested at 2

210   hours after intravesical saline infusion with vehicle or CLP290 administration. To

211   prepare fixed spinal tissues, mice were anesthetized with sodium pentobarbital

212   (50 mg/kg) and transcardially perfused with phosphate-buffered saline (PBS),

213   followed by 4% paraformaldehyde (PFA) in 0.1 M phosphate buffer. The

214   removed L6-S1 spinal cord was placed in 4% PFA for 1 day, followed by 30%

9

215   sucrose in PBS. The spinal cord was then cut into 40-µm-thick coronal sections

216   using a cryostat. We thereafter performed triple staining for c-fos, choline

217   acetyltransferase (ChAT), and KCC2. Sections were rinsed before and between

218   incubations with 0.1% Tween 20 (Sigma-Aldrich) in PBS (PBS-T). The sections

219   were incubated at room temperature for 1 hour in blocking solution (10% normal

220   212 donkey serum in PBS-T) and then at 4°C for 24 hours with primary

221   antibodies

222   diluted in PBS-T. The following primary antibodies were used: mouse anti-c-fos

223   (1:1000; Abcam), goat anti-ChAT (1:100; Sigma-Aldrich), and rabbit anti-KCC2

224   (1:300; Abcam). The following secondary antibodies were used: Alexa Fluor

225   488–conjugated donkey anti–mouse (1:1000; Abcam), Alexa Fluor 594–

226   conjugated donkey anti-goat (1:1000; Molecular Probes), and Alexa Fluor 647–

227   conjugated donkey anti-rabbit (1:1000; Molecular Probes). Slides were mounted

228   and coverslipped sections were imaged using a confocal laser microscope (TCS

229   SP9, Leica).

230

231   *Quantification*

232   In quantitative evaluations, we included five spinal cord sections from each

233   mouse, in which c-fos IHC was positive. We only selected sections with

234   ChAT-positive cells in the SPN region of the L6-S1 spinal cord because

235   preganglionic parasympathetic cholinergic neurons in the SPN region, which

236   innervate pelvic visceral organs, including the bladder, were mostly limited to the

237   L6 caudal to S1 spinal cord levels [20]. The sections selected for quantification

238   were separated by at least 80 µm to avoid duplicate counting. C-fos-positive

10

239   cells were counted in four spinal cord regions: the lateral dorsal horn (LDH),

240   medial dorsal horn (MDH), SPN, and dorsal commissure (DCM), as previously

241   reported [18]. We obtained z-stacks from every layer or region of interest

242   covering the whole thickness of the section. The number and fluorescence

243   intensity of c-fos-positive cells were measured using ImageJ software (NIH). The

244   fluorescence intensity of KCC2 was quantified as the mean value of the area

245   surrounding the cell membrane of SPN neurons using ImageJ software. We

246   subsequently measured the background intensity in each section, which was

247   defined as 100%. The fluorescence intensity of KCC2 was then divided by the

248   background intensity to calculate normalized intensity [21].

249

250   Spinal cord slice preparation

251   Acute spinal cord slices (thickness of 300 μm) were prepared from SI and

252   SCI mice (3-4 weeks old before surgery). In this experiment, we used mice at

253   younger age than those in other experiments because it was difficult to make

254   acute slice sections from matured adult mice. Slices were cut with a vibratome

255   (7000smz-2, Campden Instruments) using ice-cold cutting solution containing

256   the following (in mM): 115 N-methyl-D-glucamine-Cl, 2.5 KCl, 1.2 $NaHPO_4$, 0.5

257    $CaCl_2$, 10 $MgSO_4$, 25 $NaHCO_3$, and 25 glucose (295-305 mOsm). Slices were

258   then incubated for 10 min in the same cutting solution before being rinsed (4×)

259   with standard ACSF containing the following (in mM): 124 NaCl, 3 KCl, 1.2

260   NaH_2PO_4, 2 $CaCl_2$, 2 $MgSO_4$, 26 $NaHCO_3$, and 10 dextrose (295-305 mOsm),

261   and were then stored under continuously oxygenated conditions at room

262   temperature for approximately 1 hour.

11

263

264   Electrophysiological extracellular recordings and electrical stimulation

265   Spinal cord slices were transferred to a recording chamber and perfused (2

266   ml/min) with oxygenated (95% O_2/5% CO_2) recording ACSF solution containing

267   (in mM): 124 NaCl, 5 KCl, 2.7 $CaCl_2$, 1.3 $MgSO_4$, 1.25 NaH_2PO_4, 26 $NaHCO_3$,

268   and 10 glucose, at 30°C. Extracellular neuronal activity was recorded via a glass

269   microelectrode filled with ACSF under a microscope (BX61WI, Olympus)

270   equipped with an EMCCD camera (iXon DV887, Andor). Neuronal activity via

271   the electrodes was fed into a patch clamp amplifier (Multiclamp700B, Molecular

272   Devices). The output of the amplifier was digitized using an A/D converter

273   (Digidata 1440, Molecular Devices) with a sampling rate of 10 kHz and recorded

274   on a hard disk using data acquisition and analysis software (pCLAMP 10,

275   Molecular Devices). The firing rate of recorded neurons (spikes/s, Hz) was

276   calculated in 1-sec intervals. The dorsal root and/or LDH were stimulated once

277   every 30 s (duration of 10 ms) using a bipolar electrode to elicit the neuronal

278   firing of neurons in the SPN region. The results obtained for each group of

279   animals were normalized by the mean firing frequency during the initial 10

280   minutes after electrical stimulation. CLP290 was dissolved in 100% DMSO and

281   diluted 1000 times by ACSF to the final concentration (100 µM) just before use.

282   CLP290 was administered into the recording chamber from 20 minutes after the

283   initiation of the electrical stimulation.

284

285   Statistical analysis

286   Statistical analyses and figure generation were performed with GraphPad

12

287 prism 8 and Igor Pro 9 (Wavemetrics), and *P* < 0.05 was considered to be

288 significant. All data are reported as the mean ± SEM. All comparisons among the

289 treatments were made using a paired t-test, one-way ANOVA and Tukey's post

290 hoc analysis, the Mann-Whitney U test, and Wilcoxon rank-sum test.

291

292 **Results**

293 **Changes in cystometrograms**

294 To examine whether NVCs were affected by the activation of KCC2,

295 CLP290 was orally administered to SCI mice, and NVCs were compared before

296 and after administration (Figure 1A, B). The number of NVCs was significantly

297 lower after CLP290 administration compared to pre-administration of CLP290

298 (Figure 1C). The amplitude of NVCs was also significantly after CLP290

299 administration than that before administration (Figure 1D). Next, we compared

300 the results of cystometric analyses among 4 groups of SCI and SI mice

301 administered with vehicle or CLP290 (Figure 2). A larger number of NVCs with

302 higher amplitudes were observed in the SCI-vehicle group than in the SI-vehicle

303 group (Figure 2C, H, I). However, the number and amplitude of NVCs were

304 significantly lower in the SCI-CLP290 group than in the SCI-vehicle group

305 (Figure 2D, H, I). PVR was higher in the SCI-vehicle group than in the SI-vehicle,

306 but was not significantly altered by CLP290 (Figure 2J). No significant

307 differences were observed in ICI or MCP among the 4 groups (Figure 2E, F).

308 The administration of CLP290 to SI mice did not alter any parameters. These

309 results suggest that DO, evident as a large number of NVCs with a high

310 amplitude in SCI mice, was decreased by KCC2 activation. Since no significant

13

311 differences were observed between the SI-vehicle and SI-CLP290 groups, the

312 following histological and electrophysiological experiments used only the

313 SI-vehicle group for comparisons with SCI-vehicle and SCI-CLP290 groups.

314

315 **Changes in *c-fos* expression**

316   To confirm whether the activation of spinal cord neurons involved in DO

317 was reduced by the administration of CLP290, c-fos expression in the L6-S1

318 spinal cord following intravesical saline instillation for 2 hours was compared

319 among SI-vehicle, SCI-vehicle, and SCI-CLP290 groups. We divided each spinal

320 cord section into four regions: LDH, MDH, SPN, and DCM, and counted the

321 number of c-fos-positive cells in each region (Figure 3A). The number of

322 c-fos-positive neurons was higher in all 4 regions in the SCI-vehicle group than

323 in the SI-vehicle group. In comparisons between the SI-vehicle and SCI-CLP290

324 groups, the number of c-fos-positive cells was still increased significantly in the

325 MDH and DCN regions, but not in the LDH or SPN region in the SCI-CLP290

326 group, indicating that the CLP290 treatment reduced bladder distention-induced

327 neuronal activity in the latter two regions in SCI mice. We also confirmed that the

328 number of c-fos-positive cells showed the greatest difference between the

329 SCI-vehicle and SI-vehicle groups in the SPN region (Figure 3B-E), which

330 contains parasympathetic preganglionic neurons innervating the lower urinary

331 tract [19].

332   Since the greatest changes in neural activity after SCI were observed in

333 the SPN region, we evaluated c-fos expression in ChAT-positive preganglionic

334 parasympathetic neurons in the SPN region of the L6-S1 spinal cord. KCC2

14

335 co-expression in ChAT- and c-fos-positive neurons in the SPN region was also

336 examined to establish whether KCC2 contributed to the therapeutic effects of the

337 CLP290 treatment on DO in SCI mice. KCC2 immunoreactivity was observed in

338 ChAT-positive parasympathetic preganglionic cells in the SPN region in all

339 groups (Figure 3F-H). The number of ChAT-positive cells was similar among the

340 3 groups; however, the co-expression of c-fos and ChAT, which was higher in the

341 SCI-vehicle group than in the SI-vehicle group, was significantly lower in the

342 SCI-CLP290 group than in the SCI-vehicle group (Figure 3I, J). We then

343 compared the normalized fluorescence intensity of KCC2 in cells co-expressing

344 ChAT and c-fos. The normalized fluorescence intensity of KCC2 was lower in the

345 SCI-vehicle group than in the SI-vehicle group, but was significantly higher in the

346 SCI-CLP290 group than in the SCI-vehicle group (Figure 3K), indicating that the

347 CLP290 treatment restored the down-regulation of KCC2 induced by SCI in

348 preganglionic parasympathetic neurons located at the SPN region.

349

350 **Functional effects of KCC2 on neuronal activity in the SPN region**

351 To establish whether the activation of KCC2 by CLP290 directly altered

352 neural activity in the SPN region, neuronal firing properties were evaluated

353 extracellularly in SPN neurons using L6-S1 spinal cord slice preparations (Figure

354 4A). The locations of recorded neurons were optically confirmed after each

355 recording, and neurons outside the SPN region were excluded from the results

356 (Figure 4B). Little is known about neural activity in the SPN region of SI mice

357 although a recent study demonstrated that capsaicin activation of primary

358 afferents induced excitatory currents in mouse lumbosacral preganglionic

15

359   neurons identified by retrograde axonal transport using patch clamp recordings

360   [22]. Therefore, we compared neural activity recorded from the SPN region of SI

361   and SCI mice. Recordings were started without an electrical stimulation for the

362   first 20 minutes, and a stimulation was then applied to the dorsal root or horn of

363   the spinal cord section in order to activate afferent inputs to SPN neurons

364   (Figure 4C). In the absence of the electrical stimulation, the baseline firing

365   frequency recorded from SCI mice was slightly higher than that from SI mice

366   (Figure 4C, D). However, following the electrical stimulation in SCI mice, the

367   firing frequency at 30 to 40 minutes was significantly higher than that during the

368   initial 0 to 10 minutes without the stimulation. In contrast, SI mice did not show

369   any changes in the firing frequency over time (Figure 4D). These results suggest

370   that SPN neurons in SCI mice increased their excitability in response to afferent

371   inputs conveyed through dorsal roots. To clarify whether this increased

372   excitability was due to the altered expression of KCC2, we investigated the

373   effects of CLP290, a potent KCC2 activator, on responses to the electrical

374   stimulation in SCI mice. CLP290 was applied to a recording chamber 20 minutes

375   after the electrical stimulation was started. The normalized firing frequency of

376   SPN neurons at 40 to 60 minutes was significantly lower in the SCI-CLP290

377   group than in the SCI control group (Figure 4E, F). These results suggest that

378   the increased excitability of SPN neurons was at least partly due to the

379   decreased activity of KCC2.

380

381   **Discussion**

382   Our results showed that SCI-induced DO is associated with

16

383   downregulation of KCC2 in ChAT-positive preganglionic parasympathetic
384   neurons in the L6-S1 spinal cord, and that activation of KCC2 transporters by
385   CLP290 can reduce DO, increase KCC2 expression in preganglionic
386   parasympathetic neurons and decrease neuronal firing of SPN neurons in SCI
387   mice. To the best of our knowledge, this is the first study to show that the
388   down-regulation of KCC2 contributed to the hyperexcitability of the efferent
389   pathway innervating the bladder that induces DO after SCI.

390   To elucidate the post-SCI neural mechanisms inducing LUTD, such as DO,
391   previous studies mostly focused on changes in bladder afferent pathways after
392   SCI. Afferent pathways innervating the bladder consist of Aδ- and C-fiber
393   afferents, and following SCI, C-fiber bladder afferent pathways become
394   hyperexcitable to reorganize the spinally-mediated micturition reflex, leading to
395   DO [3][4][23]. Furthermore, previous studies showed that C-fiber desensitization
396   by the administration of capsaicin to SCI rats and mice significantly reduced the
397   number of NVCs without affecting the bladder capacity or reflex voiding [3][4][23],
398   suggesting that capsaicin-sensitive C-fiber afferent pathways play a major role in
399   the initiation of DO, whereas voiding detrusor contractions are still triggered by
400   Aδ-fiber afferents in SCI rodents. In the present study, the administration of
401   CLP290 attenuated DO, as evidenced by a reduction in NVCs during the storage
402   phase without affecting the voiding reflex because MCP, ICI, and PVR in the
403   SCI-CLP290 group were similar to those in the SI-vehicle group. Therefore, the
404   down-regulation of KCC2 appears to be involved in the enhancement of spinal
405   micturition reflexes triggered by C-fiber afferents connecting to preganglionic
406   parasympathetic efferent neurons, which induces DO without affecting voiding
407   parameters. Furthermore, SCI is known to induce urethral dysfunction, called
408   detrusor sphincter dyssynergia (DSD), during the voiding phase, leading to high
409   PVR, as also shown in this study [4]. ICI and PVR of the SCI-CLP290 group

17

410   tended to decrease compared to the SCI-vehicle group although no significant

411   difference was observed. In this study, we did not investigate SCI-induced

412   voiding dysfunctions, such as reduced voiding efficiency or DSD, which may be

413   evaluated by external urethral sphincter electromyography. Therefore, it is

414   necessary to conduct further experiments regarding this point in the future.

415   In the present study, we showed that the expression of KCC2 within the

416   SPN region of the L6-S1 spinal cord was decreased after SCI and then restored

417   by the administration of CLP290. KCC2 messenger RNA is abundantly

418   expressed in most neurons throughout the nervous system, and KCC2 is known

419   to pump out Cl^- ions in response to the influx of Cl^- via $GABA_A$ or glycine receptor

420   activation [24]. Therefore, the down-regulation of KCC2 results in high

421   intracellular Cl^- concentrations, which depolarize the Cl^- equilibrium potential,

422   leading to a decrease in inhibitory responses during $GABA_A$/glycine inhibitory

423   receptor activation, similar to that in the developmental phase [9][10]. Previous

424   studies reported that GAD and glycine levels were decreased in the L6-S1 spinal

425   cord after SCI and also that GABA receptor activation, GAD gene delivery, and

426   glycine administration attenuated DO in SCI rats [5][6][25]. The reduction of

427   inhibitory interneurons weakens the inhibitory response, but the present study

428   indicates that the down-regulation of KCC2 in ChAT-positive neurons, which

429   reduces inhibitory responses at the postsynaptic ChAT-positive neurons, play a

430   significant role in the enhanced C-fiber-to-parasympathetic spinal reflex pathway

431   responsible for DO after SCI [3][4]. Moreover, the presynaptic terminals of

432   bladder afferent nerve boutons have been shown to express GABA and/or

433   glycine immunopositivity and reach the dorsal horn and SPN in the L6-S1 spinal

434   cord [26]. Furthermore, using slice patch-clamp techniques, the electrical

435   stimulation of GABAergic interneurons was found to induce direct inhibitory

436   responses on preganglionic parasympathetic neurons in L6-S1 spinal cord slices

18

437   [15].   These data indicate that bladder afferent nerves and spinal interneurons

438   send GABAergic and/or glycinergic inputs to SPN neurons to induce inhibitory

439   neurotransmission in the normal condition. Therefore, the present study focused

440   on the plasticity of spinal efferent pathways, particularly KCC2-mediated

441   functional changes in preganglionic parasympathetic neurons in the SPN and

442   demonstrated that the down-regulation of KCC2 in cholinergic SPN neurons

443   contributed to the efferent side of neuroplasticity involved in DO after SCI.

444   Spinal cord neural circuits are reorganized following SCI, and the

445   appearance of the C-fiber-dependent, spinally-mediated micturition reflex

446   pathway causes involuntary micturition and DO [3][4]. We compared the results

447   obtained by immunostaining (c-fos and ChAT staining) and extracellular

448   recordings in the SPN region between SI and SCI mice. After SCI, a previous

449   study reported that the total number of ChAT-positive cells in the SPN region

450   was the same as that in SI mice and also that the co-expression of c-fos/ChAT

451   was increased in SCI mice [19]. Im et al. [27] showed that 82.4 ± 10.3% of

452   ChAT-positive cells were positive for c-fos in the SPN region of SCI mice. These

453   findings suggest the involvement of the excessive activation of preganglionic

454   parasympathetic cholinergic neurons in bladder efferent hyperexcitability during

455   spinal cord reorganization, which contributes to the emergence of DO after SCI.

456   However, neuronal activity in the SPN region between SI and SCI adult mice has

457   not yet been examined using electrophysiological techniques. In the present

458   study, the firing of SPN neurons during the electrical stimulation of the dorsal

459   root or spinal dorsal horn was more frequent in SCI mice than in SI mice, and the

460   bath application of CLP290 significantly reduced the firing rate from that in

461   untreated SPN cells of SCI mice.

462   The present results indicated that the single dose administration of

463   CLP290 was sufficient to modulate the activity of KCC2, which led to positive

19

464   results in immunostaining and electrophysiology experiments. CLP290 is

465   considered to be a promising pharmaceutical agent as a KCC2 activator

466   because it has been shown to induce phosphorylation of Ser940 in KCC2

467   [28][29][30]. The phosphorylation of Ser940 is known to cause membrane

468   relocation of KCC2, suggesting that CLP290 upregulates KCC2 function [31].

469   Furthermore, in the present study, the single dose administration of CLP290

470   increased the protein expression of KCC2 in ChAT-positive preganglionic

471   parasympathetic neurons, possibly due to the cell membrane insertion of

472   transporter proteins after the activation of KCC2. Further studies are needed to

473   elucidate the mechanisms underlying the effects of CLP290 on the activation of

474   KCC2 in bladder efferent pathways.

475   There are some limitations that need to be addressed, which were

476   mainly technical issues. We measured the activity of putative preganglionic

477   parasympathetic neurons in SPN region using extracellular recordings without

478   verifying whether they were cholinergic neurons or if CLP290-induced changes

479   in neuronal activity were dependent on GABAergic or glycinergic inputs.

480   Furthermore, the mechanisms inducing the down-regulation of KCC2 in SPN

481   neurons after SCI remain unknown even though previous studies demonstrated

482   that brain-derived neurotropic factor (BDNF) may contribute to the

483   down-regulation of KCC2 in the spinal cord of SCI rats with spasticity [14] and

484   also that spinal BDNF protein expression was increased in the L6-S1 spinal cord

485   of SCI mice with LUTD [32]. Therefore, future studies are warranted to

486   investigate KCC2 mechanisms, such as interactions with BDNF, which may be

487   involved in SCI-induced LUTD, including voiding dysfunction.

488   In conclusion, this is the first study to show that the down-regulation of

489   KCC2 was involved in bladder efferent hyperexcitability, which induces DO in

490   SCI mice, and also that the activation of KCC2 effectively suppressed the

20

491 excessive activity of parasympathetic preganglionic neurons in the L6-S1 spinal

492 cord and attenuated DO after SCI. Therefore, the administration of KCC2

493 activators, such as CLP290, have potential as new therapeutic agents for the

494 treatment of SCI-induced DO by targeting bladder efferent pathways.

495

496 **Compliance with ethical standards**

497 **Conflicts of interest** All authors have declared no conflicts of interest.

498

21

518   for helpful discussion and comments on the manuscript. We also thank Dr.

519   Makoto Goda (Advanced Research Facilities and Services of Hamamatsu

520   University School of Medicine) for assistance with imaging and image analyses.

521

522
523

524 **References**

525 1. Homma Y, Yoshida M, Seki N, Yokoyama O, Kakizaki H, Gotoh M,

526   Yamanishi T, Yamaguchi O, Takeda M, Nishizawa O. Symptom assessment

527   tool for overactive bladder syndrome--overactive bladder symptom score.

528   Urology 68:318-323, 2006. doi:10.1016/j.urology.2006.02.042.

529 2. Gillespie JI. A developing view of the origins of urgency: the importance of

530   animal models. BJU Int 1: 22-28, 2005. doi:

531   10.1111/j.1464-410X.2005.05652.x.

532 3. de Groat WC, Griffiths D, Yoshimura N. Neural control of the lower urinary

533   tract. Compr Physiol. Compr Physiol 5: 327-396, 2015. doi:

534   10.1002/cphy.c130056.

535 4. Wada N, Karnup S, Kadekawa K, Shimizu N, Kwon J, Shimizu T, Gotoh D,

536   Kakizaki H, de Groat WC, Yoshimura N. Current knowledges and novel

537   frontiers in lower urinary tract dysfunction after spinal cord injury- Basic

538   research perspectives. Urological Science 33: 101-113, 2022. doi:

539   10.4103/uros.uros_31_22.

540 5. Miyazato M, Sasatomi K, Hiragata S, Sugaya K, Chancellor MB, de Groat

541   WC, Yoshimura N. GABA receptor activation in the lumbosacral spinal cord

542   decreases detrusor overactivity in spinal cord injured rats. J Urol 179:

543   1178-1183, 2008. doi: 10.1016/j.juro.2007.10.030.

544 6. Miyazato M, Sugaya K, Nishijima S, Ashitomi K, Morozumi M, Ogawa Y.

545   Dietary glycine inhibits bladder activity in normal rats and rats with spinal

546   cord injury. J Urol 173:314-317, 2005. doi:

547   10.1097/01.ju.0000141579.91638.a3.

23

548   7. Toyoda H, Ohno K, Yamada J, Ikeda M, Okabe A, Sato K, Hashimoto K,

549   Fukuda A. Induction of NMDA and GABAA receptor-mediated Ca2+

550   oscillations with KCC2 mRNA downregulation in injured facial motoneurons.

551   J Neurophysiol 89: 1353-1362, 2003. doi: 10.1152/jn.00721.2002.

552   8. Yamada J, Okabe A, Toyoda H, Kilb W, Luhmann HJ, Fukuda A. Cl- uptake

553   promoting depolarizing GABA actions in immature rat neocortical neurones

554   is mediated by NKCC1. J Physiol 557: 829-841, 2004. 10.1113/jphysiol.

555   2004. 062471.

556   9. Watanabe M, Zhang J, Mansuri MS, Duan J, Karimy JK, Delpire E, Alper SL,

557   Lifton RP, Fukuda A, Kahle KT. Developmentally regulated KCC2

558   phosphorylation is essential for dynamic GABA-mediated inhibition and

559   survival. Sci Signal 12: eaaw9315, 2019. doi: 10.1126/scisignal.aaw9315.

560   10. Rivera C, Voipio J, Payne JA, Ruusuvuori E, Lahtinen H, Lamsa K, Pirvola U,

561   Saarma M, Kaila K. The K+/Cl- co-transporter KCC2 renders GABA

562   hyperpolarizing during neuronal maturation. Nature 397: 251-255, 1999. doi:

563   10.1038/16697.

564   11. Coull JA, Boudreau D, Bachand K, Prescott SA, Nault F, Sík A, De Koninck P,

565   De Koninck Y. Trans-synaptic shift in anion gradient in spinal lamina I

566   neurons as a mechanism of neuropathic pain. Nature 424: 938-942, 2003.

567   doi: 10.1038/nature01868.

568   12. Shimizu-Okabe C, Okabe A, Kilb W, Sato K, Luhmann HJ, Fukuda A.

569   Changes in the expression of cation-Cl- cotransporters, NKCC1 and KCC2,

570   during cortical malformation induced by neonatal freeze-lesion. Neurosci

571   Res 59: 288-295, 2007. doi: 10.1016/j.neures.2007.07.010.

24

572   13. Shimizu-Okabe C, Tanaka M, Matsuda K, Mihara T, Okabe A, Sato K, Inoue

573   Y, Fujiwara T, Yagi K, Fukuda A. KCC2 was downregulated in small neurons

574   localized in epileptogenic human focal cortical dysplasia. Epilepsy Res 93:

575   177-184, 2011. doi: 10.1016/j.eplepsyres.2010.12.008.

576   14. Boulenguez P, Liabeuf S, Bos R, Bras H, Jean-Xavier C, Brocard C, Stil A,

577   Darbon P, Cattaert D, Delpire E, Marsala M, Vinay L. Down-regulation of the

578   potassium-chloride cotransporter KCC2 contributes to spasticity after spinal

579   cord injury. Nat Med 16: 302-307, 2010. doi: 10.1038/nm.2107.

580   15. Araki I. Inhibitory postsynaptic currents and the effects of GABA on visually

581   identified sacral parasympathetic preganglionic neurons in neonatal rats. J

582   Neurophysiol 72:2903-2910, 1994. doi: 10.1152/jn.1994.72.6.2903.

583   16. Karnup S. Spinal interneurons of the lower urinary tract circuits. Auton

584   Neurosci 235:102861, 2021. doi: 10.1016/j.autneu.2021.102861.

585   17. Gagnon M, Bergeron MJ, Lavertu G, Castonguay A, Tripathy S, Bonin RP,

586   Perez-Sanchez J, Boudreau D, Wang B, Dumas L, Valade I, Bachand K,

587   Jacob-Wagner M, Tardif C, Kianicka I, Isenring P, Attardo G, Coull JA, De

588   Koninck Y. Chloride extrusion enhancers as novel therapeutics for

589   neurological diseases. Nat Med 19: 1524-1528, 2013. doi:

590   10.1038/nm.3356.

591   18. Vizzard MA. Increased expression of spinal cord Fos protein induced by

592   bladder stimulation after spinal cord injury. Am J Physiol Regul Integr Comp

593   Physiol 279:295-305, 2000. doi: 10.1152/ajpregu.2000.279.1.R295.

594   19. Birder LA, de Groat WC. Increased c-fos expression in spinal neurons after

595   irritation of the lower urinary tract in the rat. J Neurosci 12: 4878-4889, 1992.

596   doi: 10.1523/JNEUROSCI.12-12-04878.1992.

597 20. Fuller-Jackson JP, Osborne PB, Keast JR. Regional Targeting of Bladder

598   and Urethra Afferents in the Lumbosacral Spinal Cord of Male and Female

599   Rats: A Multiscale Analysis. eNeuro 8: 0364-21, 2021.doi:

600   10.1523/ENEURO.0364-21.2021.

601 21. Kakizawa K, Watanabe M, Mutoh H, Okawa Y, Yamashita M, Yanagawa Y,

602   Itoi K, Suda T, Oki Y, Fukuda A. A novel GABA-mediated

603   corticotropin-releasing hormone secretory mechanism in the median

604   eminence. Sci Adv 2: e1501723, 2016. doi: 10.1126/sciadv.1501723.

605 22. Kawatani M, de Groat WC, Itoi K, Uchida K, Sakimura K, Yamanaka A,

606   Yamashita T, Kawatani M. Downstream projection of Barrington's nucleus to

607   the spinal cord in mice. J Neurophysiol 126:1959-1977, 2021. doi:

608   10.1152/jn.00026.2021.

609 23. Kadekawa K, Majima T, Shimizu T, Wada N, de Groat WC, Kanai AJ, Goto M,

610   Yoshiyama M, Sugaya K, Yoshimura N. The role of capsaicin-sensitive

611   C-fiber afferent pathways in the control of micturition in spinal-intact and

612   spinal cord-injured mice. Am J Physiol Renal Physiol 313: 796-804, 2017.

613   doi: 10.1152/ajprenal.00097.2017.

614 24. Kanaka C, Ohno K, Okabe A, Kuriyama K, Itoh T, Fukuda A, Sato K. The

615   differential expression patterns of messenger RNAs encoding K-Cl

616   cotransporters (KCC1,2) and Na-K-2Cl cotransporter (NKCC1) in the rat

617   nervous system. Neuroscience 10: 933-946, 2001. doi:

618   10.1016/s0306-4522(01)00149-x.

619 25. Miyazato M, Sugaya K, Goins WF, Wolfe D, Goss JR, Chancellor MB, de

620   Groat WC, Glorioso JC, Yoshimura N. Herpes simplex virus vector-mediated

621   gene delivery of glutamic acid decarboxylase reduces detrusor overactivity

622   in spinal cord-injured rats. Gene Ther 16: 660-668, 2009. doi:

623   10.1038/gt.2009.5.

624 26. Park SK, Devi AP, Bae JY, Cho YS, Ko HG, Kim DY, Bae YC. Synaptic

625   connectivity of urinary bladder afferents in the rat superficial dorsal horn and

626   spinal parasympathetic nucleus. J Comp Neurol 15: 3002-3013, 2019. doi:

627   10.1002/cne.24725.

628 27. Im YJ, Hong CH, Jin MH, Lee BH, Han SW. c-fos expression in

629   bladder-specific spinal neurons after spinal cord injury using pseudorabies

630   virus. Yonsei Med J 49: 479-485, 2008. doi: 10.3349/ymj.2008.49.3.479.

631 28. Ferrini F, Lorenzo LE, Godin AG, Quang ML, De Koninck Y. Enhancing

632   KCC2 function counteracts morphine-induced hyperalgesia. Sci Rep 7: 3870,

633   2017. doi: 10.1038/s41598-017-04209-3.

634 29. Lizhnyak PN, Muldoon PP, Pilaka PP, Povlishock JT, Ottens AK. Traumatic

635   Brain Injury Temporal Proteome Guides KCC2-Targeted Therapy. J

636   Neurotrauma 36: 3092-3102, 2019. doi: 10.1089/neu.2019.6415.

637 30. Sullivan BJ, Kipnis PA, Carter BM, Shao LR, Kadam SD. Targeting

638   ischemia-induced KCC2 hypofunction rescues refractory neonatal seizures

639   and mitigates epileptogenesis in a mouse model. Sci Signal. 14: eabg2648,

640   2021. doi: 10.1126/scisignal.abg2648.

641 31. Lee HH, Walker JA, Williams JR, Goodier RJ, Payne JA, Moss SJ. Direct

642   protein kinase C-dependent phosphorylation regulates the cell surface

643   stability and activity of the potassium chloride cotransporter KCC2. J Biol

27

644   Chem. 282:29777-84, 2007. doi: 10.1074/jbc.M705053200.

645   32. Wada N, Shimizu T, Shimizu N, Kurobe M, de Groat WC, Tyagi P, Kakizaki H,

646   Yoshimura N. Therapeutic effects of inhibition of brain-derived neurotrophic

647   factor on voiding dysfunction in mice with spinal cord injury. Am J Physiol

648   Renal Physiol 1305-1310, 2019. doi: 10.1152/ajprenal.00239.2019.

649

650   Figure legends

651

652   **Figure1. Changes in cystometrograms before and after oral administration**

653   **of CLP290 to SCI mice.**

654   (A-B), Representative cystometrograms (CMG) before and after the

655   administration of CLP290 to SCI mice (n=10). Black arrows indicate voiding

656   contractions. Asterisks indicate NVCs. (A) Before administration of CLP290 to

657   SCI mice. (B) After administration of CLP290 to SCI mice. (C)   The number of

658   NVCs was significantly lower in the after administration of CLP290 than in the

659   before administration of CLP290. (D) The amplitude of NVCs was also

660   significantly lower in the after administration of CLP290 than in the before

661   administration of CLP290. SCI; spinal cord injury, NVC; non-voiding contraction,

662   ### P <0.001, paired t-test.

663

664   **Figure2. Comparison of cystometrograms among 4 experimental groups**

665   **with or without oral administration of CLP290.**

666   (A-D), Representative cystometrograms (CMG) after oral administration of

667   vehicle or CLP290 to SI and SCI mice. Black arrows indicate voiding

668   contractions. Asterisks indicate NVCs. (A) Vehicle administration to SI mice. (B)

669   CLP290 administration to SI mice. The administration of CLP290 to SI mice did

670   not alter any parameter. (C) Vehicle administration to SCI mice. (D) CLP290

671   administration to SCI mice. The number and amplitude of NVCs decreased.

672   (E-J), Results of CMG parameters among 4 groups (n=10 in each). (E, F) There

673   was no significant difference in ICI or MCP among the 4 groups. (G) IVBP was

674   higher in the SCI-vehicle group than in the SI-vehicle group. (H) The number of

675   NVCs was significantly lower in the SCI-CLP290 group than in the SCI-vehicle

676   group. (I) The amplitude of NVCs was also significantly lower in the SCI-CLP290

29

677   group than in the SCI-vehicle group. (J) PVR was significantly increased in the

678   SCI-vehicle and SCI-CLP290 groups.

679   SI; spinal cord intact, SCI; spinal cord injury, NVC; non-voiding contraction, ICI;

680   intercontraction interval, MCP; maximum voiding bladder contraction pressure,

681   IVBP; intravesical baseline pressure, NVC; non-voiding contraction, PVR;

682   post-void residual urine volume. # P <0.05, ### P <0.001, One-way ANOVA and

683   Tukey's post hoc analysis.

684

685   **Figure3. Changes of c-fos, ChAT and KCC2 expression in the spinal cord**

686   **among 4 experimental groups with or without oral administration of**

687   **CLP290.**

688   Immunohistochemistry of the L6/S1 segment. (A) Illustration of each segment of

689   the spinal cord. The scale bar is 200 μm. (B-E) Comparison of c-fos-positive cell

690   counts in the LDH, SPN, MDH, and DCN regions. The number of c-fos-positive

691   cells was significantly increased in the SCI-vehicle group, particularly in the SPN

692   region. (F-H) Comparison of c-fos-, ChAT-, and KCC2-positive cells in the SPN

693   region. KCC2 expression was confirmed on the cell membrane in all three

694   groups. Red circles show ChAT-positive cells, and yellow circles show c-fos- and

695   ChAT-positive cells. Scale bars are 50 μm. (I) Comparison of the number of

696   ChAT-positive cells in the SPN region. There was no significant difference in the

697   number of ChAT-positive cells among the three groups. (J) Percentage of

698   co-expression of c-fos- and ChAT-positive cells. The co-expression of c-fos- and

699   ChAT-positive cells was significantly higher in the SCI-vehicle group than in the

700   SI-vehicle group,   but was significantly lower in the SCI-CLP290 group than in

701   the SCI-vehicle group. (K) Normalized intensity of KCC2. KCC2 was lower in the

702   SCI-vehicle group than in the SI vehicle group. KCC2 was higher in the

703   SCI-CLP290 group than in the SCI-vehicle group.

30

704   LDH; lateral dorsal horn, SPN; sacral parasympathetic nucleus, MDH; medial

705   dorsal horn, DCN; dorsal commissural nucleus, KCC2; K^+-Cl^- co-transporter 2;

706   ChAT; choline acetyltransferase. # $p<0.05$, ### $p<0.001$ One-way ANOVA and

707   Tukey's post hoc analysis.

708

709   **Figure4. Functional effects of KCC2 activation on neuronal activity in the**

710   **SPN region.**

711   (A) Example recordings of firing transitions in the SPN region of the L6/S1 spinal

712   cord segment. An action potential in the arrow is expanded and shown on the

713   right panel. (B) The stimulation electrode was located in the dorsal horn, and the

714   recording electrode on the external side of the SPN region. The scale bar is 200

715   μm. (C, D) In each recording, it was confirmed whether the stimulation electrode

716   was located in the SPN region. In cells in the SPN region of SCI mice, the firing

717   frequency was increased during the stimulation. At 30 to 40 minutes, the firing

718   frequency in SCI mice after the stimulation was higher than that before the

719   stimulation and was also significantly higher than that in SI mice. (E, F) At 40 to

720   60 minutes, the CLP290-administered group showed a lower normalized

721   frequency than that in the control group. The frequency of each recording was

722   normalized with an average value in the range of 0.5 to 10 minutes.

723   Data are presented as the ±standard error of the mean (±SEM). * $p<0.05$ (vs 0 to

724   10 min), # $p<0.05$ (SI mice vs SCI mice), && $p<0.01$ (CLP290 vs control), the

725   Mann-Whitney U test and the Wilcoxon rank-sum test.

726

Figure 1.
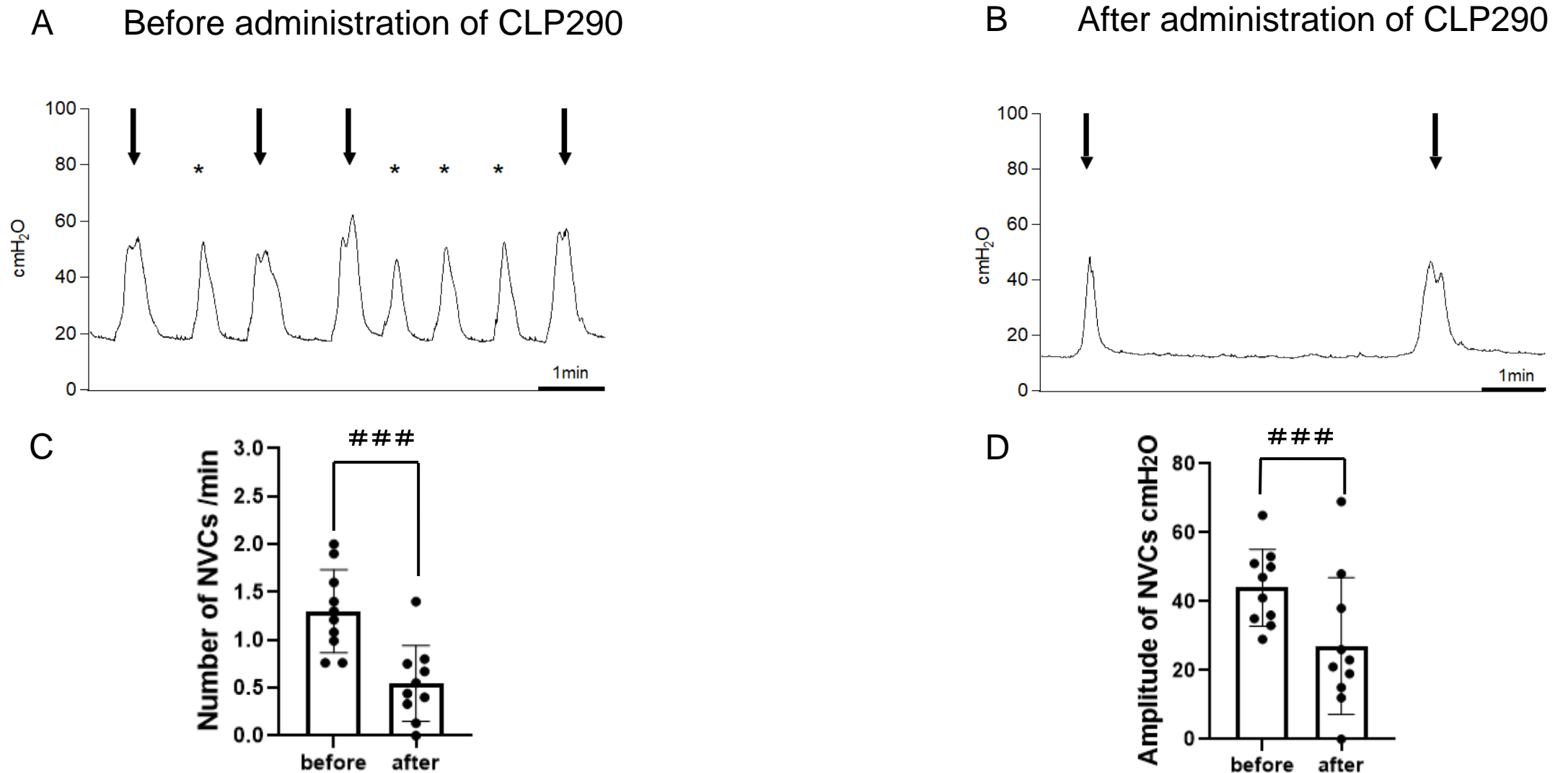
A   Before administration of CLP290

B   After administration of CLP290

C

D

Figure1. Changes in cystometrograms before and after oral administration of CLP290 to SCI mice.
(A-B), Representative cystometrograms (CMG) before and after the administration of CLP290 to SCI mice (n=10). Black arrows indicate voiding contractions. Asterisks indicate NVCs. (A) Before administration of CLP290 to SCI mice. (B) After administration of CLP290 to SCI mice. (C) The number of NVCs was significantly lower in the after administration of CLP290 than in the before administration of CLP290. (D) The amplitude of NVCs was also significantly lower in the after administration of CLP290 than in the before administration of CLP290. SCI; spinal cord injury, NVC; non-voiding contraction. ### P <0.001, paired t-test.
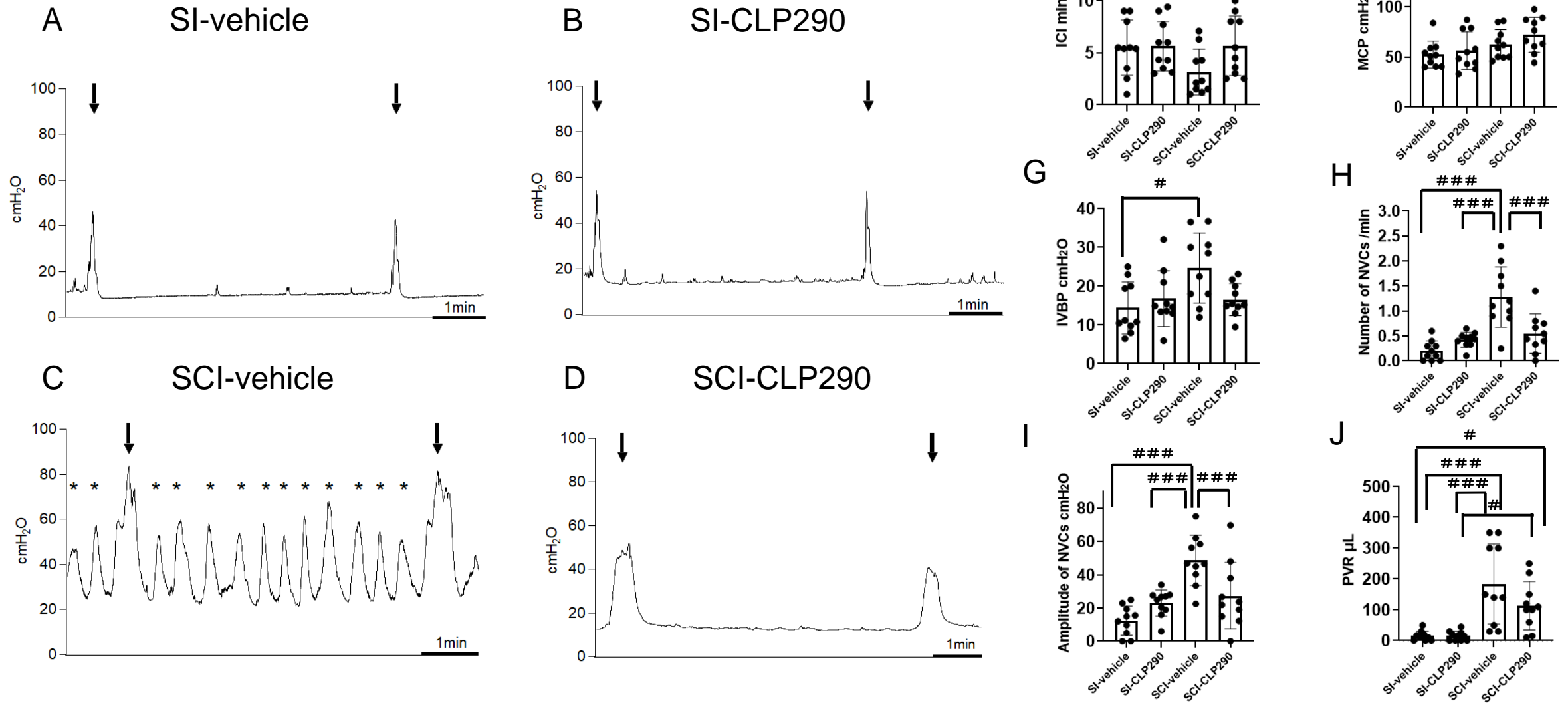
Figure2. Comparison of cystometrograms among 4 experimental groups with or without oral administration of CLP290.
(A-D), Representative cystometrograms (CMG) after oral administration of vehicle or CLP290 to SI and SCI mice. Black arrows indicate voiding contractions. Asterisks indicate NVCs. (A) Vehicle administration to SI mice. (B) CLP290 administration to SI mice. The administration of CLP290 to SI mice did not alter any parameter. (C) Vehicle administration to SCI mice. (D) CLP290 administration to SCI mice. The number and amplitude of NVCs decreased. (E-J), Results of CMG parameters among 4 groups (n=10 in each). (E, F) There was no significant difference in ICI or MCP among the 4 groups. (G) IVBP was higher in the SCI-vehicle group than in the SI-vehicle group. (H) The number of NVCs was significantly lower in the SCI-CLP290 group than in the SCI-vehicle group. (I) The amplitude of NVCs was also significantly lower in the SCI-CLP290 group than in the SCI-vehicle group. (J) PVR was significantly increased in the SCI-vehicle and SCI-CLP290 groups.
SI; spinal cord intact, SCI; spinal cord injury, NVC; non-voiding contraction, ICI; intercontraction interval, MCP; maximum voiding bladder contraction pressure, IVBP; intravesical baseline pressure, NVC; non-voiding contraction, PVR; post-void residual urine volume. # P <0.05, ### P <0.001, One-way ANOVA and Tukey's post hoc analysis.

Figure 3.
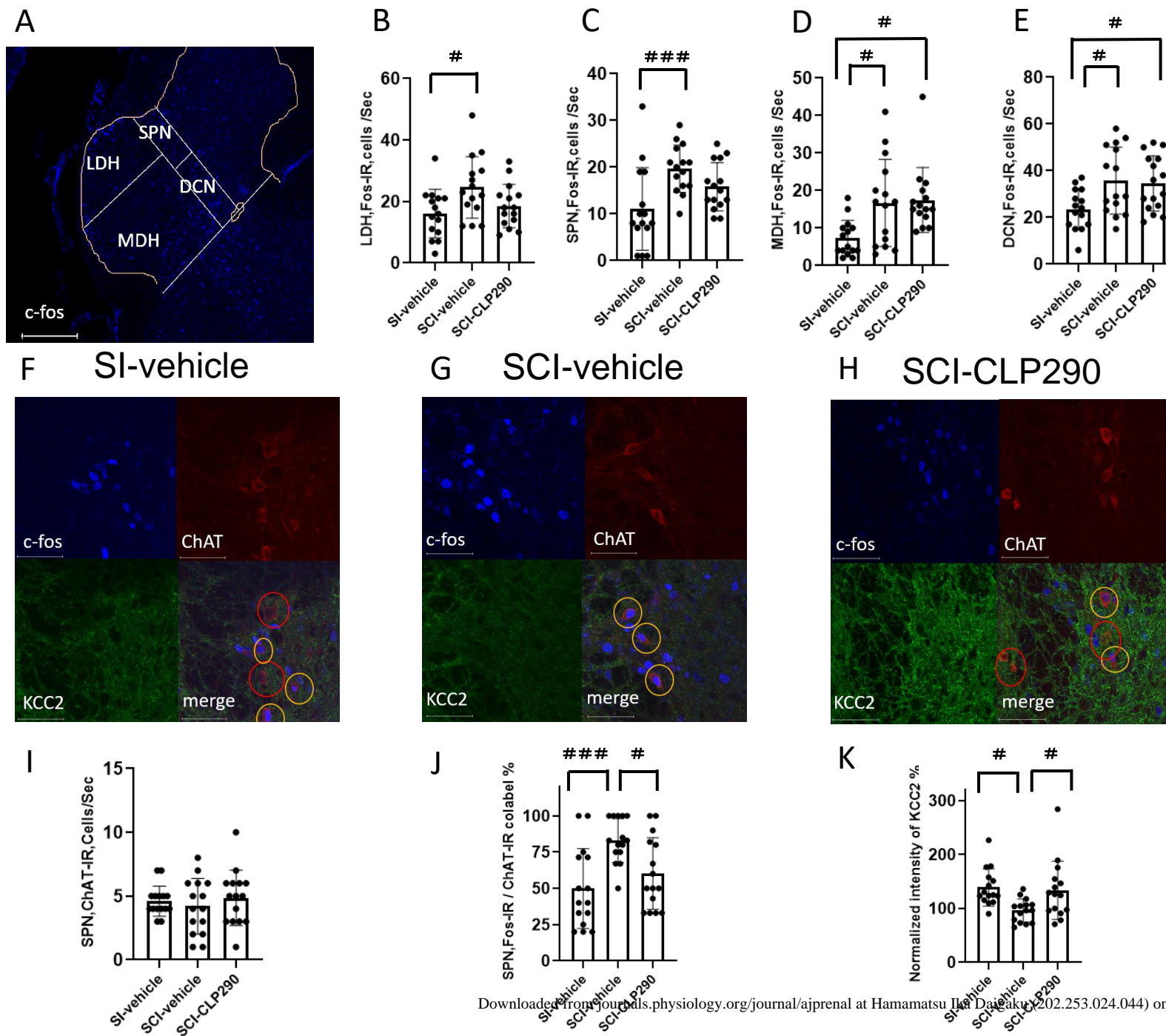
Figure3. Changes of c-fos, ChAT and KCC2 expression in the spinal cord among 4 experimental groups with or without oral administration of CLP290. Immunohistochemistry of the L6/S1 segment. (A) Illustration of each segment of the spinal cord. The scale bar is 200 μm. (B-E) Comparison of c-fos-positive cell counts in the LDH, SPN, MDH, and DCN regions. The number of c-fos-positive cells was significantly increased in the SCI-vehicle group, particularly in the SPN region. (F-H) Comparison of c-fos-, ChAT-, and KCC2-positive cells in the SPN region. KCC2 expression was confirmed on the cell membrane in all three groups. Red circles show ChAT-positive cells, and yellow circles show c-fos- and ChAT-positive cells. Scale bars are 50 μm. (I) Comparison of the number of ChAT-positive cells in the SPN region. There was no significant difference in the number of ChAT-positive cells among the three groups. (J) Percentage of co-expression of c-fos- and ChAT-positive cells. The co-expression of c-fos- and ChAT-positive cells was significantly higher in the SCI-vehicle group than in the SI-vehicle group, but was significantly lower in the SCI-CLP290 group than in the SCI-vehicle group. (K) Normalized intensity of KCC2. KCC2 was lower in the SCI-vehicle group than in the SI vehicle group. KCC2 was higher in the SCI-CLP290 group than in the SCI-vehicle group.

LDH; lateral dorsal horn, SPN; sacral parasympathetic nucleus, MDH; medial dorsal horn, DCN; dorsal commissural nucleus, KCC2; K+-Cl− co-transporter 2; ChAT; choline acetyltransferase. # $p<0.05$, ### $p<0.001$ One-way ANOVA and Tukey's post hoc analysis.

Figure 4.
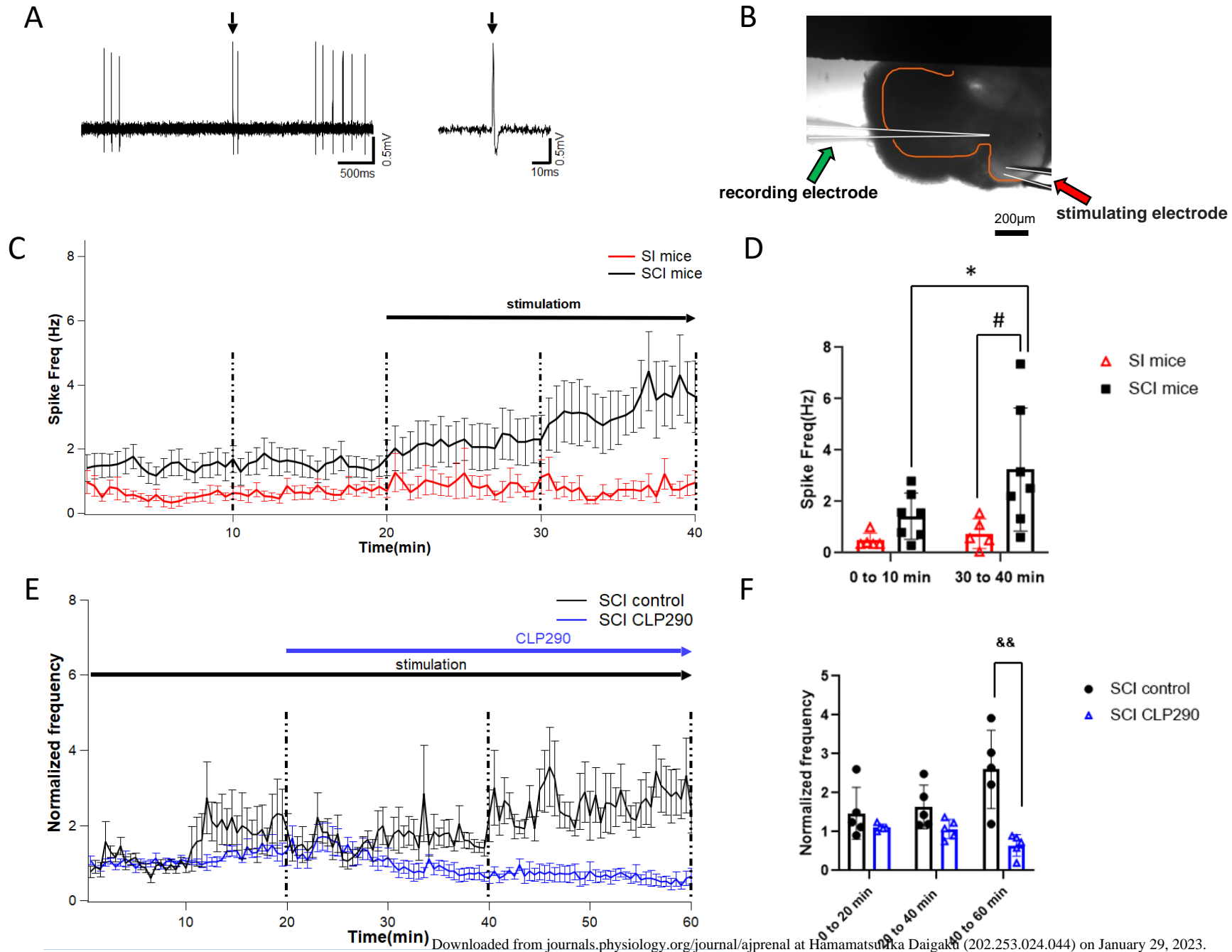
Figure4. Functional effects of KCC2 activation on neuronal activity in the SPN region.

(A) Example recordings of firing transitions in the SPN region of the L6/S1 spinal cord segment. An action potential in the arrow is expanded and shown on the right panel. (B) The stimulation electrode was located in the dorsal horn, and the recording electrode on the external side of the SPN region. The scale bar is 200 μm. (C, D) In each recording, it was confirmed whether the stimulation electrode was located in the SPN region. In cells in the SPN region of SCI mice, the firing frequency was increased during the stimulation. At 30 to 40 minutes, the firing frequency in SCI mice after the stimulation was higher than that before the stimulation and was also significantly higher than that in SI mice. (E, F) At 40 to 60 minutes, the CLP290-administered group showed a lower normalized frequency than that in the control group. The frequency of each recording was normalized with an average value in the range of 0.5 to 10 minutes. Data are presented as the ±standard error of the mean (±SEM). * $p<0.05$ (vs 0 to 10 min), # $p<0.05$ (SI mice vs SCI mice), && $p<0.01$ (CLP290 vs control), the Mann-Whitney U test and the Wilcoxon rank-sum test.

Therapeutic effects of KCC2 activation on detrusor overactivity in mice with spinal cord injury

METHODS

SCI was produced by the Th8-9 spinal cord transection in female C57BL/6 mice. At 4 weeks after SCI, CLP290, a KCC2 activator was administered, and cystometry was performed. Thereafter, neuronal activity with c-fos staining and KCC2 expression in the cholinergic preganglionic parasympathetic neurons in the SPN were examined using immunohistochemistry. In a separate group of animals, firing properties of neurons in the SPN region were evaluated by extracellular recordings in spinal cord slice preparations.

OUTCOME
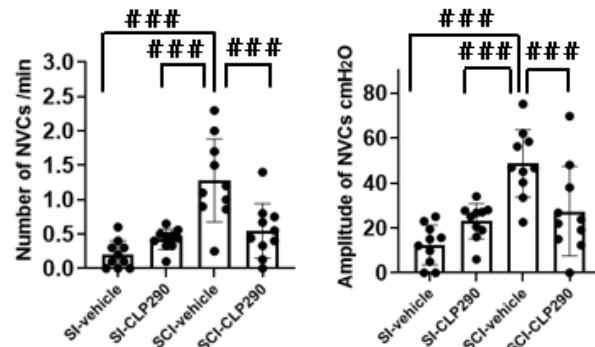
DO evident as non-voiding contractions (NVC) was significantly reduced by CLP290 treatment in SCI mice.

Electrode   SPN region
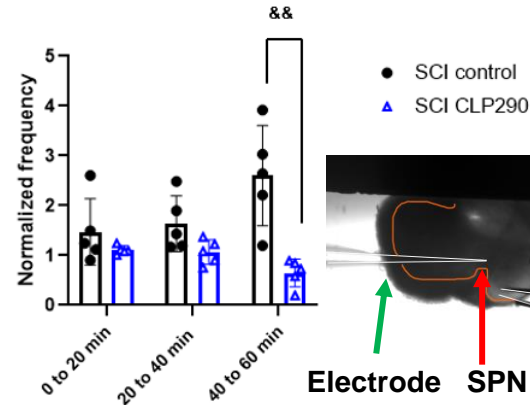
CLP290 administration suppressed the high frequency firing activity of SPN neurons in SCI mice.
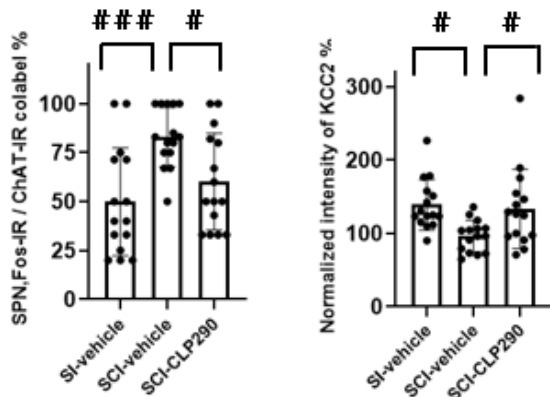
The number of c-fos-positive cells and co-expression of c-fos in choline acetyltransferase (ChAT)-positive cells were decreased in the SPN region of SCI-CLP290 group vs. SCI-vehicle group. KCC2 immunoreactivity was present on the cell membrane of SPN neurons, and the normalized fluorescence intensity of KCC2 in ChAT-positive SPN neurons was decreased in SCI-vehicle group, vs. SI-vehicle group, but recovered in SCI-CLP290 group.

CONCLUSION

These results suggest that activation of KCC2 chloride ion transporter may be a therapeutic modality for the treatment of SCI-induced DO by targeting bladder efferent pathways.